LIMNOLOGY and OCEANOGRAPHY

ASLO

Limnol. Oceanogr. 64, 2019, 785–802

doi: 10.1002/lno.11074

Fine scale depth regulation of invertebrate larvae around coastal fronts

Nicolas Weidberg [1,2,a*] **Wayne Goschen,** [3,4] **Jennifer M. Jackson,** [2,5] **Paula Pattrick,** [2,3] **Christopher D. McQuaid,** [1] **Francesca Porri** [1,2]

[1]Department of Zoology and Entomology, Rhodes University, Grahamstown, South Africa
[2]South African Institute for Aquatic Biodiversity, Grahamstown, South Africa
[3]South African Environmental Observation Network, Elwandle Coastal Node, Nelson Mandela University Ocean Sciences Campus, Port Elizabeth, South Africa
[4]Institute for Coastal and Marine Research, Nelson Mandela University, Port Elizabeth, South Africa
[5]Hakai Institute, Victoria, British Columbia, Canada

Abstract

Vertical migrations of zooplankters have been widely described, but their active movements through shallow, highly dynamic water columns within the inner shelf may be more complex and difficult to characterize. In this study, invertebrate larvae, currents, and hydrographic variables were sampled at different depths during and after the presence of fronts on three different cruises off the southern coast of South Africa. Internal wave dynamics were observed in the hydrographic data set but also through satellite imagery, although strong surface convergent currents were absent and thermal stratification was weak. During the first two cruises, fronts were more conspicuous and they preceded strong onshore currents at depth which developed with the rising tide. Vertical distributions of larvae changed accordingly, with higher abundances at these deep layers once the front disappeared. The third cruise was carried out during slack tides, the front was not conspicuous, deep strong onshore currents did not occur afterward and larval distributions did not change consistently through time. Overall, the vertical distributions of many larval taxa matched the vertical profiles of shoreward currents and multivariate analyses revealed that these flows structured the larval community, which was neither influenced by temperature nor chlorophyll. Thus, the ability to regulate active vertical positioning may enhance shoreward advection and determine nearshore larval distributions.

Diel vertical migrations of zooplankters across the world's oceans have been studied since the development of sonar in the 20th century revealed the magnitude of this phenomenom (Barham 1963; Heywood 1996; Fornshell and Tesei 2013). The main selective pressures thought to cause these 24 h vertical displacements are visual predation and metabolic rates as both would be too high in clear, relatively warm surface waters during the day (Enright 1977; Stich and Lampert 1981). Although widespread throughout the planktonic community, diel vertical migration is known to be highly variable and responsive to organismal physiological condition (Hays et al. 2001) and prevailing environmental forcing (Weidberg et al. 2015), thus it can be combined with other active behaviors across the water column. When studied in shallower waters over the continental shelves, however, other more complex patterns of vertical movements emerged. For coastal meroplankters, most patterns seem related to offshore advection, which is an important selective pressure on pelagic organisms specific to coastal regions (Jackson and Strathmann 1981). For coastal plankton, and especially for the larvae of coastal benthic invertebrates, offshore transport may be a source of mortality and could result in recruitment failure, where not enough larvae settle to replace the adult population. Thus, by swimming against the weak vertical flows imposed by upwelling–downwelling transitions and other hydrographical processes, coastal plankton can remain at depths where currents are directed onshore (Queiroga and Blanton 2004; Genin et al. 2005; Shanks and Shearman 2009).

The ability to regulate their depth allows coastal plankton and larvae to respond to nearshore hydrographical structures such as fronts. Fronts can be defined as oceanographic features that separate two different water types and present a typical vertical current structure. Many different invertebrate larvae have been observed to accumulate at fronts by first being horizontally transported to them and then by swimming against

*Correspondence: j_weidberg@hotmail.com or nlo009@uit.no

[a]Present address: Department of Arctic Marine Biology, University of Tromso, Tromso, Norway

Additional Supporting Information may be found in the online version of this article.

the downward vertical flow which characterizes these convergent structures (Franks 1992; Pineda 1999; Shanks et al. 2000; Weidberg et al. 2014). Fronts can be formed by multiple hydrographical processes operating at different spatio-temporal scales including Ekman forcing, estuarine circulation, tides, and topographically driven currents (Le Fevre 1986; Shanks et al. 2003). Processes that cause accumulation at these fronts, like internal waves and upwelling, may become crucial for benthic larval aggregation. In particular, convergent features produced by internal wave fronts and their associated bores have been shown to promote the aggregation and shoreward transport of invertebrate larvae (Pineda 1999; Helfrich and Pineda 2003; Weidberg et al. 2014). These internal motions are usally caused by tidal forcing over abrupt topographies at the shelf break which causes instabilities that travel along the thermocline (Pond and Pickard 1983; Holloway 1987). The potential onshore displacement of larval accumulations driven by internal waves may have profound consequences for the final recruitment of individuals into the adult populations as suggested by the positive association of frontal occurrence and larval settlement (Lagos et al. 2008; Woodson et al. 2012). It is, however, difficult to establish the importance of fronts on larval dispersal as it may depend on their frequency, persistence, strength, and seasonal interaction with larval biological features (Largier 1993). In addition, in the case of internal tidal waves, there might also be shoreward transport at depth, when the typical foam lines and slicks are not visible at the surface (Pineda 1991; Lievana MacTavish et al. 2016).

Along the south coast of South Africa (Fig. 1), there are a variety of processes which are known to generate fronts at many different scales, times, and locations. A major mesoscale frontal feature separates the shelf Agulhas Bank waters from the warm core of the Agulhas Current (Lutjeharms 2006). In addition, Ekman forcing is not the only source of upwelled waters in the region: fast flow velocities typical of the Agulhas Current and its meanders onto the shelf cause shelf edge upwelling, semi-permanent upwelling cells and their associated fronts (Schumann et al. 1982; Goschen and Schumann 1990; Lutjeharms et al. 2000; Goschen et al. 2015). Internal waves have also been observed across the Agulhas Bank (Largier and Swart 1987; Jackson et al. 2012). All these structures can potentially affect the distributions of a wide invertebrate larval community with highly adaptive active responses. Fronts have been hypothesized to influence the distribution of mussel larvae in the region (McQuaid and Phillips 2000) and high abundances were associated with internal wave fronts over the Agulhas Bank (Porri et al. 2014; Weidberg et al. 2015).

In this study, we sampled larval distributions around frontal structures within the inner shelf waters off the south coast of South Africa. Our sampling methodology allowed the physical characterization of the events in an attempt to identify the physical drivers behind their development. In addition, as we sampled during and after frontal occurrence, we were able to quantify for the first time the persistence of frontal larval distributions, a key feature that can allow us to evaluate the long-term effects of coastal fronts on larval transport, settlement and population dynamics.

Materials and methods

Field samplings

On three different days during the austral spring of 2014 (25 September, 06 October, and 29 October, hereafter Events 1, 2, and 3, respectively), nearshore waters off Sardinia Bay (34.03–34.07°S, 25.47–25.51°E) on the western exposed side of Cape Recife (Fig. 1) were surveyed in search of foam lines and/or oily slicks parallel to the coast on board the 13 m long R/V *uKwabelana*. In addition, LANDSAT imagery was also retrieved for the same days at the area surveyed to observe the same surface structures (Supporting Information). Once the front was located by observing foam lines or oily slicks, a total of six stations were set. These were arranged as two cross-frontal transects (A and B), each with one station at the front, one between the front and the shore (250–700 m from the front), and one on the seaward (at 200–700 m from the front) side of the front. These stations were defined as frontal, onshore, and offshore stations, respectively. At each station, a SBE19 plus conductivity - temperature- depth probe (CTD) with a Wetlabs ECO-AFL fluorometer was lowered from the surface to the bottom and the temperature profiles obtained were inspected in search of a rapid drop in temperature with depth (approximately 1°C/5 m) pointing to the presence of a thermocline. A 2.2 KC Denmark 23.580 plankton pump with a net of 60 μm mesh size was deployed three times; once at 1 m depth, once at the thermocline (or at mid-depths in the absence of a thermocline), and once 2–3 m above the bottom to collect the biological larval samples. The pump filtered at each depth for about 7 min which yielded a mean volume of 1.3 m^3 (between 0.9 m^3 and 2.3 m^3). At the same time, an acoustic Doppler current profiler (ADCP) Teledyne RD Instruments Workhorse Monitor of 300 kHz frequency, beam angle 20° and a 4-beam system was deployed facing downward, at 0.5 m depth, on the port side of the boat for a minimum of 30 min. The instrument registered currents in three axes (E-W, N-S, and vertical) every 0.5 m by emitting one ping every 1.5 s and using one ping to calculate one individual measurement or ensemble. It also recorded bottom tracking to account for boat drift. The six stations sampled took about 3–4.5 h (Time 1, front present). Once the front dissipated, the same sampling design was repeated at or close to the initial stations (3.5–4.5 h, Time 2, front dissipated).

Physical variables

Cross-shore profiles for temperature and chlorophyll *a* (Chl *a*) were obtained from the CTD and fluorometer sensors at each transect for each event during and after the presence of the front. CTD and fluorometer data were processed with

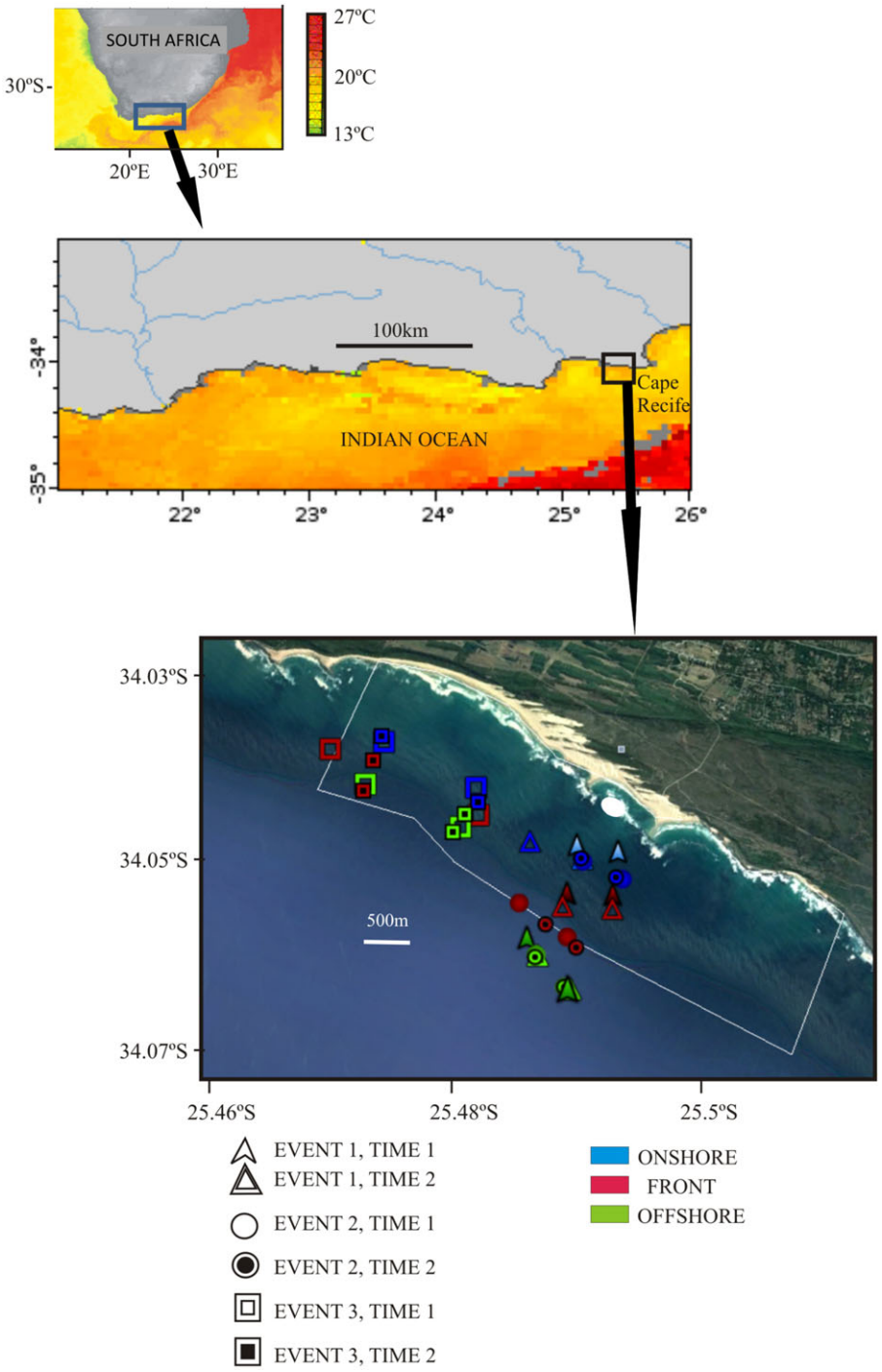

Fig. 1. Maps of the study site. A scale of sea surface temperature is presented for the general maps. In the high resolution Google Earth map, all sampling stations are shown. The white line delimits the marine protected area of Sardinia Bay. [Color figure can be viewed at wileyonlinelibrary.com]

Seabird's Seasoft V2 software, using the standard steps recommended for the SBE 19 Plus. ADCP profiles were collected at the same stations and these data were processed. The processing steps used included subtracting bottom tracking velocities, discarding data with less than 100% good criteria, discarding data where the velocity error was greater than 40 cm s^{-1} and discarding estimates of mean currents calculated with less than 100 counts per 0.5 m depth cell. Currents were then averaged over the total time of deployment at a given station (between 30 min and 45 min).

Hourly measurements of wind direction and velocity during the cruises were obtained from the South African Weather

Service (SAWS) at Port Elizabeth International Airport, 12 km to the northeast. Speeds were corrected for height using the wind profile power law (Hsu et al. 1994) to get estimates at 9 m following the same procedure applied for the region in previous studies (Weidberg et al. 2015). From these data, an upwelling index as zonal Ekman transport was calculated (Bakun 1973) with positive and negative values to indicate offshore and onshore displacements of surface waters, respectively. In addition, tidal motions were retrieved at Port Elizabeth with the programme WXTide32 with a time resolution of 10 min. Tidal ranges in the region span approximately 0.4–2 m.

Plankton samples

The cod end of the plankton pump was rinsed with filtered seawater and its contents was poured into 250 mL plastic jars into which 95% ethanol was added. These samples were inspected in the laboratory with a microscope (Zeiss Stemi DV4) to identify the larvae of benthic invertebrates. We identified all larvae to the lowest taxonomic category possible, family and stages in the case of barnacles. Organisms were counted through the whole sample and their numbers were divided by the total volume filtered to standardize abundances as individuals per m^3.

Frontal circulation

Given the orientation of the coast, the North–South axis was considered a good proxy of shoreward–seaward directions. Thus, from the velocity estimates obtained with the ADCP, the cross-shore-meridional currents at those depths at which plankton abundances were sampled were used to infer accumulation speeds. Subsequently, accumulation speeds (velocities at which particles may accumulate at either side of the front; *see* Pineda 1999; Weidberg et al. 2014 for details) were calculated as:

$$\Delta\mathrm{Von} = \mathrm{Vf} - \mathrm{Von}$$

$$\Delta\mathrm{Voff} = \mathrm{Voff} - \mathrm{Vf}$$

where Von, Voff, and Vf are cross-shore speeds at onshore, offshore, and frontal waters, with positive values indicative of northward, onshore direction. These were vertically averaged for each 0.5 m binned depth, horizontally averaged for each onshore, frontal, and offshore pair of stations. These calculations were done during and after frontal development (Times 1 and 2, respectively) thus enabling the estimation of a net difference between times for both the onshore and offshore sides of the front as:

$$\Delta\mathrm{Von}\,(\mathrm{T2}-\mathrm{T1}) = \Delta\mathrm{VonT2} - \Delta\mathrm{VonT1}$$

$$\Delta\mathrm{Voff}\,(\mathrm{T2}-\mathrm{T1}) = \Delta\mathrm{VoffT2} - \Delta\mathrm{VoffT1}$$

Statistics

In order to infer the accumulation patterns of larvae around fronts, the abundances of the most abundant taxa (those with a minimum of 3 ind m^{-3} at one station at a given depth) were used as dependent variables in factorial ANOVAs, with position (onshore, front, or offshore) and depth (surface, middle, or bottom) as fixed factors. As variances for the interaction between position and depth were often heterogeneous (Levene's test $p < 0.05$), abundances were log transformed. To ensure that samples were independent within each ANOVA, for each taxon and event, separate analyses were carried out during frontal occurrence (Time 1) and after frontal dissipation (Time 2).

A proxy of larval vertical positioning in the water column was calculated as the mean larval depth (MLD; Tapia et al. 2010), which is a mean of depths sampled at a given station weighted by the respective larval abundances:

$$\mathrm{MLD} = \sum(N_i \times D_i)/\sum N_i$$

where N_i is larval abundances at depth D_i (surface, middle, or bottom) and $\sum N_i$ is the total number of larvae at the station. These calculations were done at stations where larvae reached at least 3 ind m^{-3} at one depth. Similarly, we also obtained a mean depth weighted by cross-shore currents V (MVD) as

$$\mathrm{MVD} = \sum(V_i \times D_i)/\sum V_i$$

where V_i is cross-shore flows at depth D_i (from the surface to the bottom every 0.5 m) and $\sum V_i$ is the summation of flows through the water column. For these calculations, flows were rescaled by subtracting the maximum negative value (i.e., the fastest seaward current) from all values at a given station so that all resultant values were positive. Then, to infer how the vertical dynamic structure of the cross-shore flow affected vertical larval distributions, MLDs were regressed against MVDs by means of ordinary least square (OLS) regression for the most abundant taxa. The variance explained by these regressions (R^2) was used as a proxy of the degree of coupling between larval and cross-shore flows distributions for a specific taxon.

Multivariate principal component analyses (PCAs) were performed from averages of the most important physical variables, after normalization, for every larval taxon: temperature (T), Chl *a* (CHLA), depth (D), and velocities for the three axes: North–South (U), East–West (V), and vertical (Z). This procedure allowed insight into which physical variables most influenced the structure of the larval community. Three different PCAs were carried out with means of the physical variables calculated for all samplings (Time1 + Time 2); for sampling during Time 1 only; and those done during Time 2 only. Correlations between physical variables were examined for each

PCA and if a pair of variables presented a Pearson's R value greater than 0.8, one of them was removed from the analysis to avoid excessive multicollinearity (Clarke and Gorley 2006). The Pc1 of these analyses was considered as a descriptor of larval assemblages and its taxon specific values were correlated with the R^2 of the relationships between MLDs and MVDs. In addition, larval swimming velocities obtained from the literature (Chia et al. 1984; Weidberg et al. 2014) were represented for all multivariate analyses to establish any potential relationship with larval active locomotion.

Results

Field sampling

The frontal structures observed off Sardinia Bay in 2014 on 25 September, 06 October, and 29 October (hereafter Events 1, 2, and 3, *see* Fig. 1) shared some visual characteristics. On the first two dates, several surface slicks parallel to the shore were observed and the most conspicuous and closest to shore was sampled. This pattern was especially evident during Event 2, with five consecutive narrow foam structures approximately 100 m apart observed at the beginning of the sampling period. These foam structures were confirmed by LANDSAT images (Supporting Information). In addition, fish activity was observed at the surface within the slicks and Sandwich terns (*Thalasseus sandvicensis*) were flying around the front (pers. obs.). During Event 3, a single 100 m wide slick was observed which did not move shoreward and did not present any foam.

Physical variables

Wind forcing was relatively weak during our cruises, with winds never exceeding velocities of 7 m s^{-1} or absolute Ekman transport rates of 1000 m^3 km^{-1} s^{-1} (Fig. 2). This was especially evident for Events 1 and 2, while during Time 2 (front dissipated) in Event 3 stronger downwelling, westerly winds blew (Fig. 2). Spring tides occurred during Events 1 and 2, sampled 1 d after new moon and 2 d before full moon, respectively, with ranges greater than 1.5 m, while Event 3 occurred 2 d before the first quarter moon corresponding to a neap tide with a range of around 1 m. Fronts consistently occurred as tides were close to their lowest levels (during flood tides for Events 1 and 2 and during ebb tide for Event 3) while they disappeared as the tide was rising (Fig. 2).

Cross-shore contour profiles of Chl *a*, temperature, and currents revealed differences in the structure of the water column between events and times but also some similarities. During Event 1, the warmest waters were recorded close to the surface (17.4°C) and relatively cold waters (~ 14°C) were offshore at the bottom, especially during Time 1 (front present). The limited vertical differences in temperatures were not enough to form a marked thermocline. Chl *a* values were quite low, close to normal winter values for the region, never exceeding 2 mg m^{-3}. Offshore, currents around 20 m depth were flowing westward and downward, especially at transect A during Time 1 at very high velocities up to 90 cm s^{-1}, while they shifted northward during Time 2. Onshore, flows were much weaker and did not present any clear directional pattern (Fig. 3).

Event 2 was characterized by lower temperatures than during Event 1, with a narrow offshore surface layer (10 m width) of roughly 14°C that was closer to the shore at Time 2 (Fig. 4). Onshore waters around 12°C were mixed. Chl *a* values were even lower than on Event 1 and very close to 0, with slightly higher values at mid-depths. Again, strong flows at 20–25 m depth developed offshore, but this time they were directed eastward, northward and upward at speeds of 20–35 cm s^{-1} during Time 1 (front present). Closer inshore, strong bottom westward currents developed during Time 1. During Time 2 (front dissipated), currents were flowing mainly shoreward at higher speeds (50 cm s^{-1}).

During Event 3, temperatures were in general warmer than during Event 2, with a 10 m depth surface layer of 16°C and bottom waters of 12°C. At transect B, slightly colder (Time 1) and warmer (Time 2) waters occupied the whole water column at the front. Chl *a* levels were much higher than during previous events, attaining values of 6 mg m^{-3} but they did not present a clear spatial pattern. Currents were much weaker than previously recorded and the strong offshore deep currents were not present. Instead, relatively strong westward currents (20 cm s^{-1}) were flowing offshore at the surface during Time 1, but this pattern was not clear by Time 2. Bottom waters at the front were flowing seaward at similar speeds to Time 1. No clear structures were observed for vertical flows during this event (Fig. 5).

Frontal circulation

Positive relative speeds from both sides of the front, indicative of potential transport toward the front and hence possible particle accumulation, were not particularly faster at the surface than the bottom during frontal occurrence at Time 1 compared to Time 2 (Table 1). In fact, negative relative speeds occurred at some depths during the three events, with no clear temporal or spatial structure. The only clear pattern occurred at the bottom layer for Events 1 and 2, when, at Time 2, positive and stronger shoreward relative speeds developed, leading to the highest temporal differences in accumulation speeds from both sides of the front (between 15 cm s^{-1} and 48 cm s^{-1}, Table 1). Thus, for Events 1 and 2, the weakening of the front might be related to the appearance of stronger bottom landward flows.

Plankton samples and statistics

A wide diversity of zooplankters was found over the three events. Barnacle larvae were separated into two broad taxonomic categories as either balanids (mainly comprising the species *Tetraclita serrata, Balanus glandula*, and some megabalanids) or chthamalids (*Octomeris angulosa* and *Chthamalus dentatus*). These larvae were also separated into different developmental stages, early nauplii (nauplii I–III), late nauplii

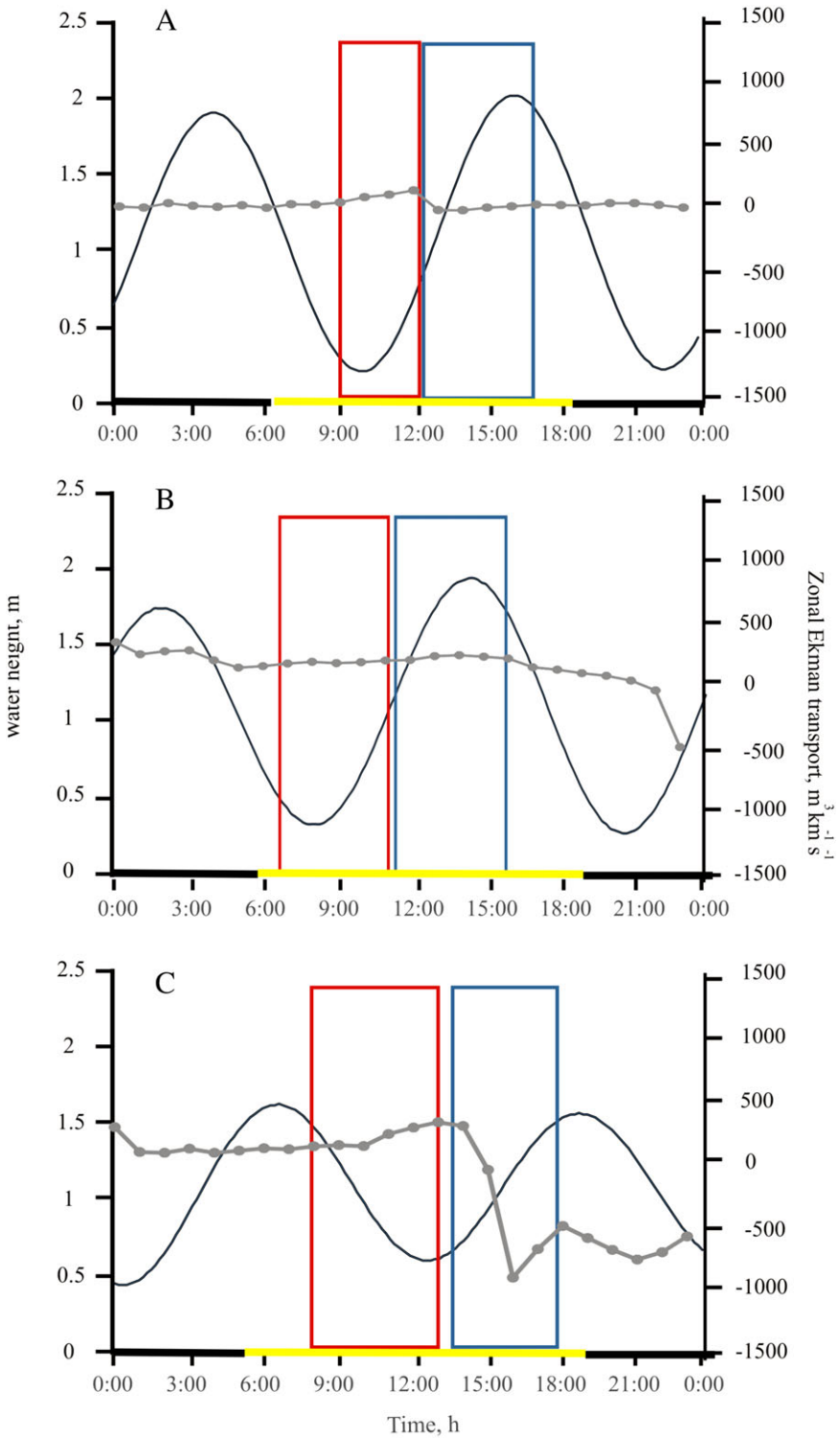

Fig. 2. Time series of tides and zonal Ekman transport for the three events on 25 September 2014 (**A**), 06 October 2014 (**B**), and 29 October 2014 (**C**). Red and blue rectangles show the times at which nearshore waters were sampled during and after the presence of fronts, respectively. On the X axis, dark and yellow lines mark night-time and daytime periods, respectively. [Color figure can be viewed at wileyonlinelibrary.com]

(IV–VI), and cyprids. Within balanid cyprids, two different morphs were found, but could not be taxonomically identified, so they were named as balanid cyprids A and B. *O. angulosa* could only be identified and separated from *C. dentatus* as late nauplii. Even broader taxonomic categoríes were chosen for the rest of the groups. Decapod stages were

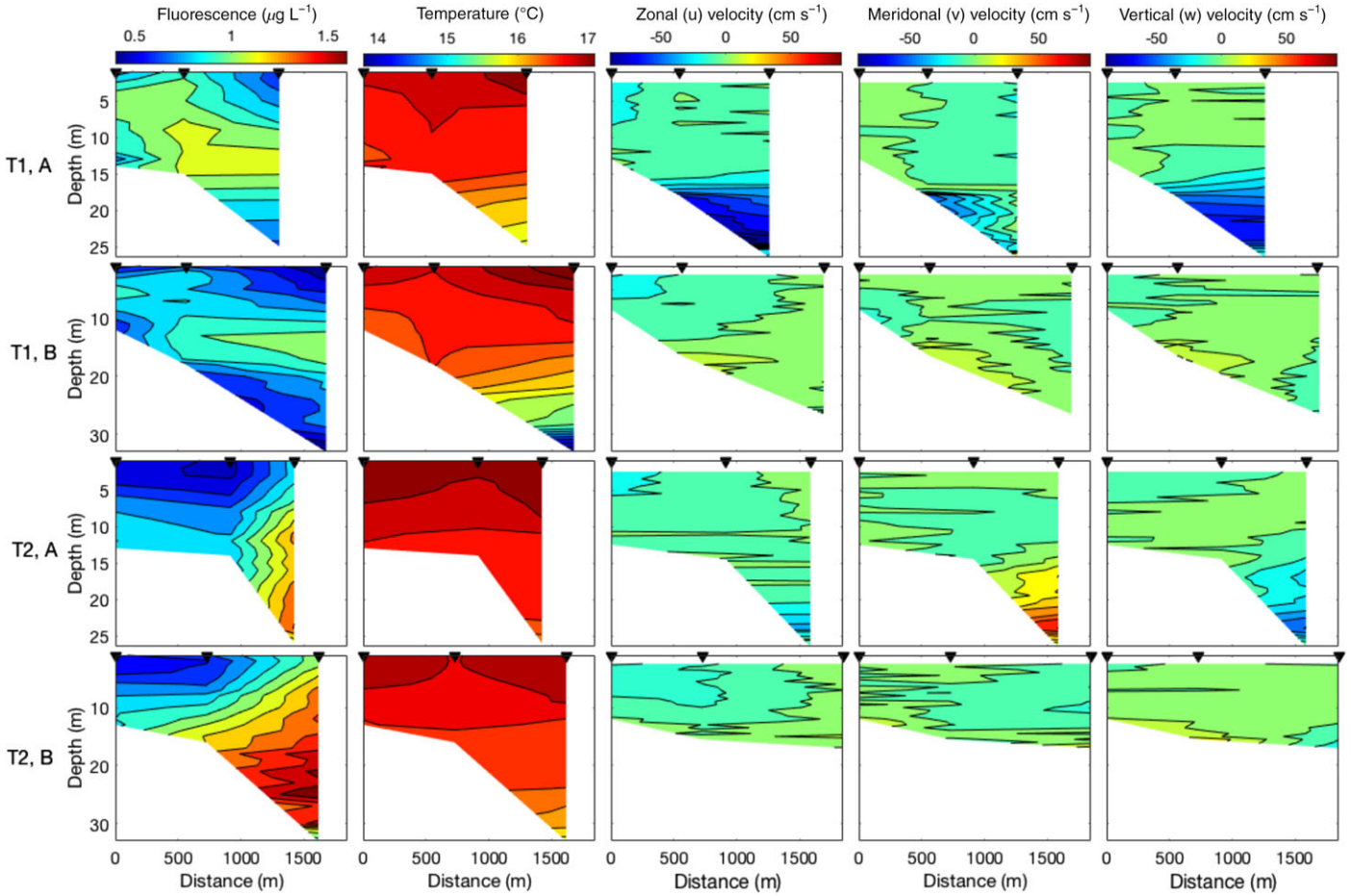

Fig. 3. Contour profiles of Chl *a*, temperature, and currents along the three axes for Event 1, along two transects (A and B), during (T1) and after frontal development (T2). Dark inverted triangles mark show the position of each sampled station. [Color figure can be viewed at wileyonlinelibrary.com]

also identified as zoeae and megalopae. Among them, there were pinnotherid and porcelanid zoeae, probably belonging to either *Porcellana* or *Pisidia*. Spionid annelids, possibly of the genus *Polydora*, could be identified and separated from other segmented annelid larvae. Bryozoan cyphonauts identified could have belonged to the *Membranipora*. Among the echinoderms, pluteus larvae of brittle stars and sea urchins could be separated.

Temporal variability in larval composition was obvious, not only between events, but also between times within events, with some taxa appearing or disappearing from coastal waters within a few hours (Table 2). Specific analyses of variance for each taxon occurring at each event and time revealed that depth and the interaction depth × position significantly affected larval abundances more than position of the front on its own, especially for Events 1 and 2 and Time 1 (Table 2). Most of the taxa tended to be present at higher abundances at mid-bottom layers and offshore (Table 2; Fig. 6A,C), with the clear exception of bryozoan cyphonauts which were found in greater abundances onshore and at the surface (Table 2, Fig. 6B). Interestingly, during Events 1 and 2, many taxa were located deeper (middle, Event 1 and bottom, Event 2; *see* Table 2) during Time 2 compared to their distributions at Time 1. This temporal shift was evident for balanid cyprids, late and early nauplii, chthamalid early nauplii and gastropods during Event 1; and for balanid cyprid A and early nauplii, zoeae of anomurans, pinnotherids and other brachyurans, annelids and gastropods during Event 2 (Table 2). During Event 3, while the front was present (Time 1), many taxa were abundant offshore (balanid cyprid A and late nauplii, chthamalid early nauplii, *O. angulosa* late nauplii, and anomuran zoeae) and/or were located at the bottom (all decapod taxa), but all these patterns disappeared at Time 2 (Table 2).

Correlations between MLDs and mean cross-shore flow depths differed across taxa from nonsignificant with low R^2 values in the case of bryozoans to very significant fits explaining up to 70% of variability in MLD (Fig. 7). Overall, 10 out of 13 different larval taxa showed significant correlations, while there was not a clear association in chthamalid early nauplii, pinnotherid zoeae and bryozoan cyphonauts. Larval and cross-shore currents vertical profiles were found to

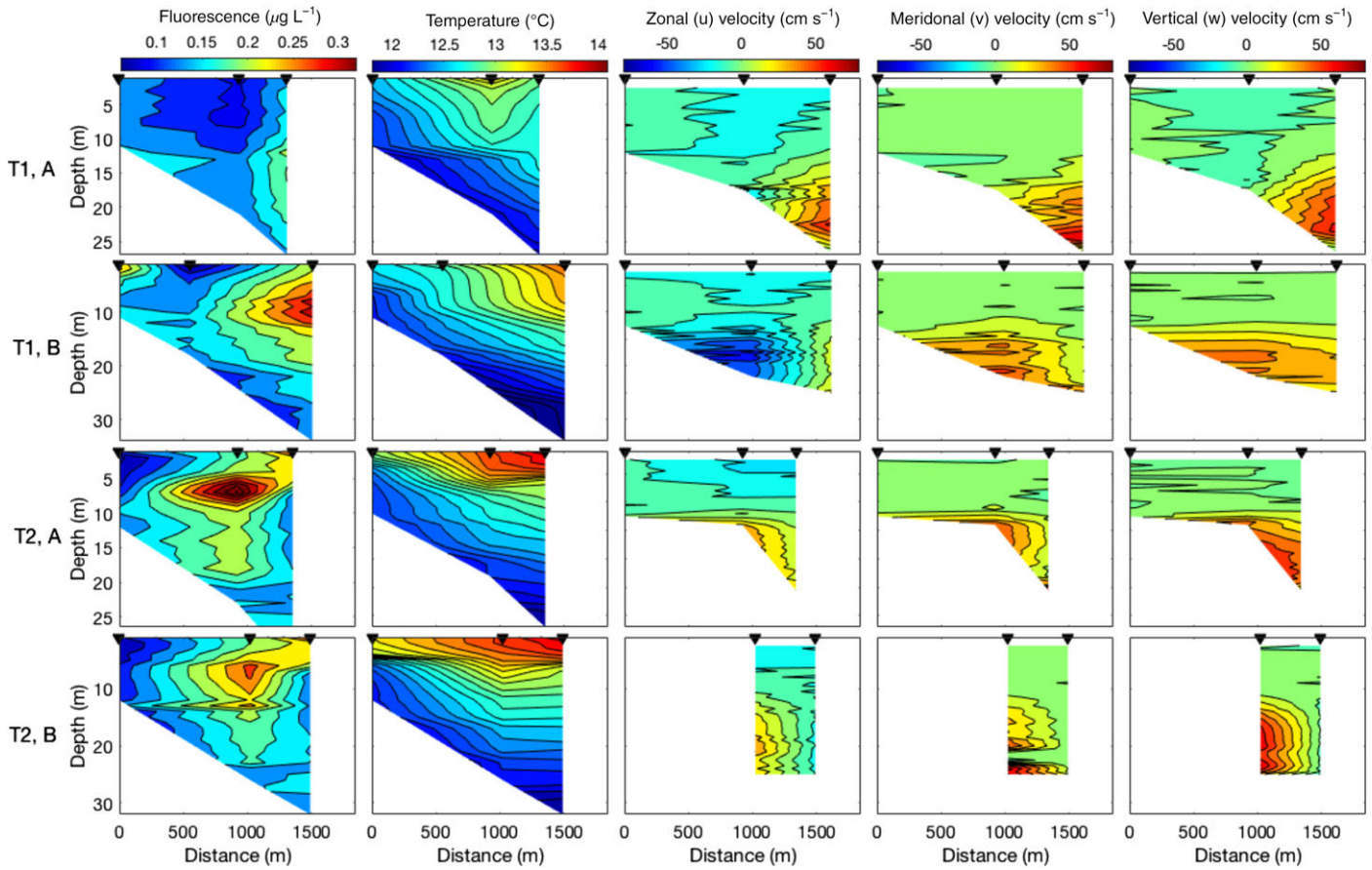

Fig. 4. Contour profiles of Chl *a*, temperature, and currents along the three axes for Event 2 along two transects (A and B) during (T1) and after frontal development (T2). Dark inverted triangles mark show the position of each station. [Color figure can be viewed at wileyonlinelibrary.com]

match at some stations for those taxa presenting high R^2, especially at Time 2 when strong shoreward currents were present (Fig. 7).

PCA multivariate analyses for all data, Time 1 and Time 2 data sets presented similar patterns, with some variations. The larval community was structured along Pc1 for all analyses, which explained 51.1%, 55.3%, and 58.8% of total variability of all data, Time 1, and Time 2 analyses, respectively (Fig. 8). The variable that contributed the most to Pc1 was always mean cross-shore speeds *V*, while the role of temperature, Chl *a*, depth, and the other vectorial components of current velocities was not as important. *V* contributed more to Pc1 when data after frontal development were considered (–0.522 compared to –0.513 for all data and – 0.475 for Time 1, Fig. 8). Pc2 explained much lower percentages of variability (not more than 21.5%) and was associated mainly with the vertical component of flow *Z* and Chl *a* (Fig. 8). The range of larval velocities spanned two orders of magnitude, from slow echinoderm pluteus larvae that typically swim 0.01 cm s^{-1} to very fast barnacle cyprids that reach several cm s^{-1} (Chia et al. 1984). PCA did not however show any effect of larval velocity on larval community structure.

For Time 2, depth had to be discarded as an input variable as it was strongly and positively correlated with *V* and presented a correlation coefficient greater than the recommended 0.8 (Clarke and Gorley 2006). Thus, taxa located deeper in the water column after frontal development experienced stronger shoreward flows (Fig. 9C). This pattern was blurred, although still significant, when all data were considered (Fig. 9A) but was not significant for the Time 1 data set (Fig. 9B). Again, these distributions were not clearly linked to larval swimming velocities, although some patterns emerged when taxonomy was considered. During frontal occurrence, barnacle cyprids and decapod mean depths were around 10 m, but these ranged from 5 m to more than 20 m after the front has passed. Also, at Time 1 nauplii, bryozoan cyphonauts and echinoderms were at depths shallower than 10 m, associated to shoreward flow. At Time 2, the same taxa remained at very similar depths, even though mean shoreward velocities were much lower than during Time 1, or even negative (Fig. 9).

A strong correspondence was found between the taxon specific Pc1 scores of the PCA for the whole data set and the goodness of fit between larval and *V* vertical distributions,

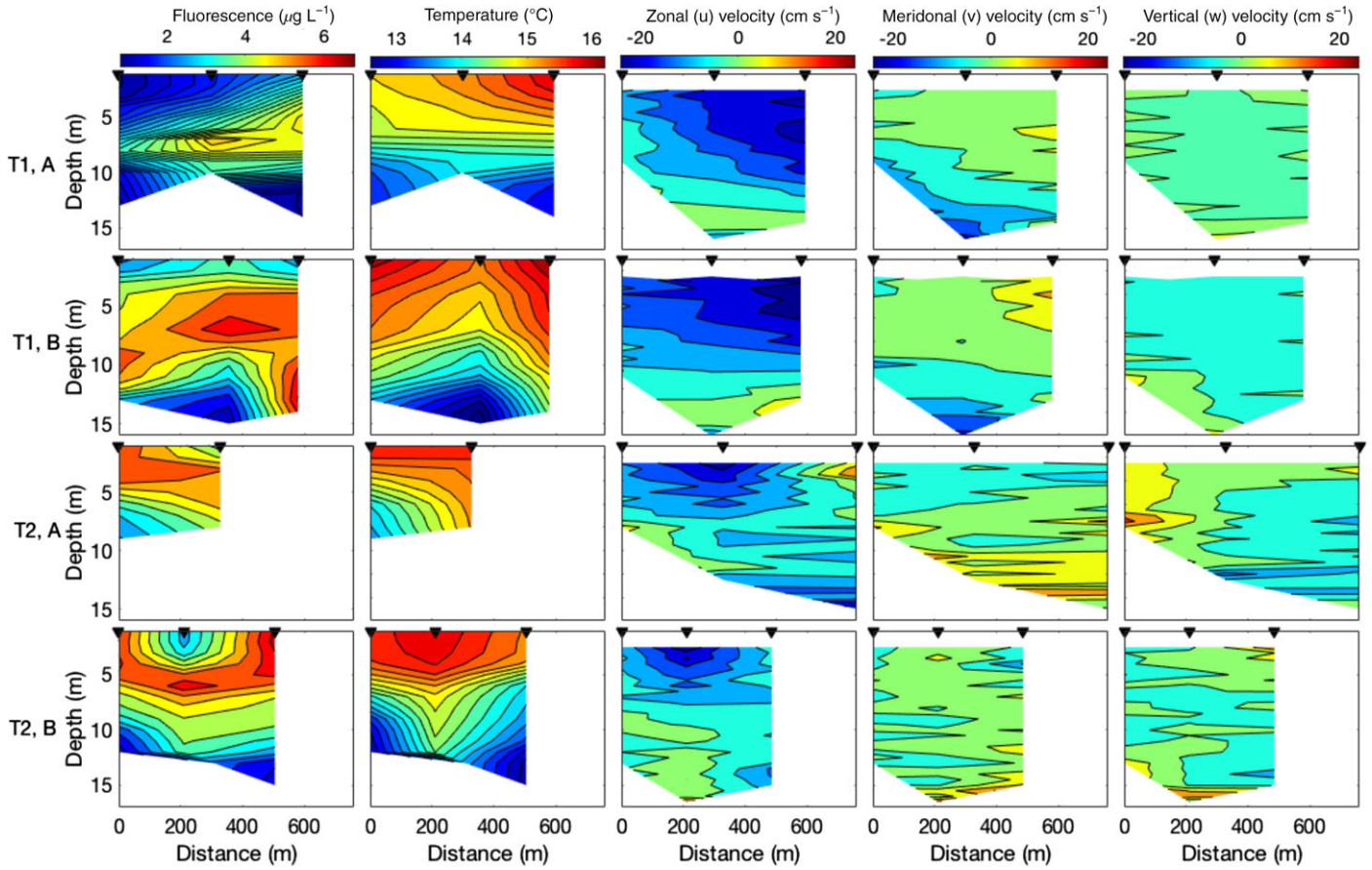

Fig. 5. Contour profiles of Chl *a*, temperature, and currents along the three axes for Event 3 along two transects (A and B) during (T1) and after frontal development (T2). Dark inverted triangles mark show the position of each station. [Color figure can be viewed at wileyonlinelibrary.com]

Table 1. Accumulation speeds in cm s^{-1} from the onshore and offshore sides for each frontal event, during (Time 1) and after (Time 2) development. Bold letters indicate positive accumulation speeds were obtained. Temporal differences (T2 − T1) are also shown.

		Time 1		Time 2			
Event	Depth	Δvon	Δvoff	Δvon	Δvoff	Δvon (T2 − T1)	Δvoff (T2 − T1)
1	Surface	**1.177**	−7.6725	−1.062	**2.2855**	−2.239	9.958
	Middle	**1.2875**	−6.831	−0.47	−0.223	−1.7575	6.608
	Bottom	−18.575	**7.117**	−2.9545	**35.146**	15.6205	28.029
2	Surface	**3.937**	**0.5125**	−1.9975	**5.205**	−5.9345	4.6925
	Middle	**7.123**	**0.2575**	−1.904	**0.258**	−9.027	0.0005
	Bottom	−44.21	−1.0065	**3.526**	**20.603**	47.736	21.6095
3	Surface	**8.1025**	**1.578**	**3.31**	−1.523	−4.7925	−3.101
	Middle	**0.1365**	**3.8415**	**2.063**	**1.528**	1.9265	−2.3135
	Bottom	−6.0725	**4.2325**	−4.09	−2.0335	1.9825	−6.266

measured as the R^2 of their corresponding regressions. Thus, the main component structuring larval community was clearly correlated with the degree of coupling between larval vertical distribution and cross-shore flow vertical profiles (Fig. 10A). This pattern was not associated with organismal velocity, with slow swimmers like bryozoans, gastropod, and bivalve veligers presenting different values of both R^2 and Pc1. On the other hand, although not significant, this degree of coupling was associated with the mean cross-shore flow (Fig. 10B). Thus, the better the coupling between larval vertical positioning and shoreward flow structure, the higher the shoreward currents experienced by larvae.

Table 2. Results of the analyses of variance performed on each larval taxon at each event at the time of front occurrence and after (Times 1 and 2, respectively). Significant effects are represented (*: $0.01 < p < 0.05$; **: $0.001 < p < 0.01$; ***: $p < 0.001$). Blank cells correspond to nonsignificant terms. Cells containing "no" show that a given taxon was not present at that event and time. Mean abundances and their standard deviations at Times 1 and 2 are shown. If interactions containing any individual factor were significant, the significance of those factors on their own was not taken into account. Besides significant terms, significant differences are shown between factor levels (on, onshore; f, front; off, offshore; s, surface; m, mid-depths; b, bottom). For the interactions, different combinations of levels are possible (i.e., off-m, offshore mid-depths) and only the combinations with the highest larval abundances are shown. The term "rest" refers to the remaining combinations of levels product of the statistical interactions not showed. Significant differences found among levels contained within the term "rest" are not represented.

Taxa	Time 1	Position	Depth	Position × Depth	Time 2	Position	Depth	Position × Depth
Event 1								
Balanid early nauplii	350.41 ± 480.91			**; off-m > rest	348.77 ± 989.66		**; m > b = s	
Chthamalid early nauplii	5.86 ± 16.52				6.97 ± 13.99		*; m ≥ b ≥ s	
Balanid late nauplii	4.24 ± 6.32			*; on-b = f-b = f-m = off-m > rest	9.58 ± 27.9		**; m > b = s	
O. angulosa late nauplii	0.35 ± 0.89					no	no	no
Balanid cyprid A	1.09 ± 1.53				1.04 ± 1.56		*; m ≥ b ≥ s	
Balanid cyprid B	1.31 ± 1.76				1.33 ± 2.71			*; off-b = off-m > rest
Brachyuran zoeae	3.56 ± 5.15		*; b = m > s		1.69 ± 2.34	**; off > f = on	***; m = b > s	
Brachyuran megalopae	0.57 ± 1	*; f = off > on	**; m > b = s			no	no	no
Porcelanid zoeae	2.2 ± 4.71			*; off-m > rest	1.92 ± 3.98	*; off ≥ f ≥ on		
Anomuran zoeae	5.15 ± 8.55		*; m ≥ b ≥ s		1.64 ± 3.29	**; off ≥ f ≥ on	*; m ≥ b ≥ s	
Pinnotherid zoeae	1.73 ± 3.07				0.93 ± 1.53			
Other annelids	79.28 ± 134.18		**; m = b > s		51.08 ± 73.31	*; off ≥ f ≥ on	**; m > b = s	
Spionid annelid	0.93 ± 1.76		*; m ≥ b ≥ s		0.2 ± 0.34			
Gastropod veligers	27.34 ± 27.2			**; m = b > f-s > rest	28.56 ± 45.61	**; off > f = on	***; m > b = s	
Bivalve veligers	139.65 ± 146.12		***; m = b > s		122.13 ± 196.17		***; m > b = s	
Bryozoans cyphonauts	4.76 ± 6.1	**; on ≥ f ≥ off	*; m = s > b		3.05 ± 4.26		**; m = s > b	
Event 2								
Balanid early nauplii	40.01 ± 135.76				44.21 ± 81.35	*; on ≥ off ≥ f	*; m ≥ b ≥ s	
Balanid late nauplii	0.9 ± 1.46			*; f-m = off-m > rest	10.12 ± 26.1			*; off-m > rest
Balanid cyprid A		no	no	no	0.86 ± 1.39		**; b > m = s	
Balanid cyprid B	1.82 ± 2.55			*; on-m = b > rest	1.06 ± 1.91	*; on ≥ f ≥ off		
Brachyuran zoeae	3.68 ± 7.71				4.58 ± 8.28	*; on > f ≥ off	**; b > m = s	
Porcelanid zoeae	0.48 ± 0.94			**; off-b = off-m > rest	0.44 ± 0.9			
Anomuran zoeae	1.04 ± 1.78		*; b ≥ m ≥ s		0.84 ± 1.29		*; b > m = s	
Pinnotherid zoeae	0.87 ± 2				1.68 ± 3.02	*; on > f ≥ off	*; b > m = s	
Other annelids	197.04 ± 230.96		***; b > m = s		147.14 ± 213.1		**; b ≥ m ≥ s	
Gastropod veligers	30.11 ± 60.76			*; b = on-m > rest	26.35 ± 54.35		**; b ≥ m ≥ s	
Bivalve veligers	49.33 ± 63.66	*; on ≥ off ≥ f	**; b ≥ m ≥ s		73.66 ± 43.95		*; b = m > s	
Bryozoans cyphonauts	0.57 ± 1.44			**; on-m > rest		no	no	no

Event 3						205.82 ± 422.21		
Balanid early nauplii	141.17 ± 364.45							
Chthamalid early nauplii	1.01 ± 2.99	*; off > f = on				3.44 ± 5.82		
Balanid late nauplii	6.67 ± 19.4	**; off > f = on				7.74 ± 12.88	*; m ≥ s ≥ b	
O. angulosa late nauplii	0.36 ± 1.16	*; off >f = on				1.1 ± 2.27		
Balanid cyprid A	5.15 ± 9.19	**; off > f = on	**; b ≥ m ≥ s			3.71 ± 3.4	*; m = b > s	
Balanid cyprid B	1.2 ± 1.49			*; off-m = b > rest		0.92 ± 0.98		
Brachyuran zoeae	5.26 ± 5.81		*; b ≥ m ≥ s			4.57 ± 4.63		
Porcelanid zoeae	1.72 ± 3.37		*; b > m = s			1.8 ± 2.59		
Anomuran zoeae	8.08 ± 12	*; off ≥ f ≥ on	*; b ≥ m ≥ s			6.91 ± 6.63		*; m = b = off-s > rest
Pinnotherid zoeae	0.98 ± 1.61		*; b ≥ m ≥ s			1.8 ± 4.64		
Other annelids	17.79 ± 44.17					33.41 ± 44.69		
Spionid annelid	1.96 ± 4.16			**; off-m > off-b > rest		2.07 ± 2.86	**; m ≥ s ≥ b	
Gastropod veligers	12.2 ± 31.34	*; off > f = on	*; b ≥ m ≥ s			19.7 ± 44	*; off ≥ f ≥ on	
Bivalve veligers	99.08 ± 275.69	**; off > f = on	*; b = m > s			88.42 ± 171.24	*; off ≥ f ≥ on	
Bryozoans cyphonauts	10.16 ± 14.5		**; s ≥ m ≥ b			8.42 ± 11.13	*; on ≥ f ≥ off	***; s > m = b
Brittle star pluteus	1.12 ± 1.83					1.12 ± 1.83		

Discussion

Field observations show that fronts developed off Sardinia Bay in austral spring of 2014 and they affected the distribution of coastal invertebrate larvae. Specifically, fronts were conspicuous as consecutive foam lines or oily slicks appearing parallel to the shore during spring tides as water level was close to its minimum. Significant surface accumulations of larvae were, however, not detected at the foam lines, in agreement with low, or even negative, accumulation speeds around the structure. On the other hand, 3–4 h later, during rising spring tides, fronts disappeared and strong shoreward flows developed at mid to bottom depths. This coincided with the presence of high-larval abundances at the same depths, in marked contrast with their previous vertical distributions during frontal occurrence. Such a shift in vertical distributions is consistent with the correspondence between larval and cross-shore flow mean depths for many taxa. High correlation observed between larval mean depths and larval mean shoreward currents (V) were only observed after frontal occurrence, however, so that V was important in explaining larval community assemblages, but only after frontal dissipation.

Physical forcing driving frontal development

The timing of appearance of both surface fronts and deeper strong shoreward currents point to tidally forced internal waves as the most likely drivers of the structures observed during our cruises. Alongshore foam lines are consistent with internal tidal bore fronts which move onshore as inshore subthermocline waters start to recede and sink (Pineda 1994, 1999; Weidberg et al. 2014). Fast shoreward mid to bottom currents typically occur at the following phase of wave development, as the next set of incoming waves approach inshore waters (Pineda 1991; Leichter et al. 1998). This temporal pattern reflects the dynamics of the internal baroclinic tide. Although baroclinic tides do not have to be in phase with surface barotropic tidal variations of sea level, the onset of strong subthermocline landward flows can coincide with rising tides, especially if these are marked (Leichter et al. 1998), thus being in opposite phase compared with usual estuarine circulation. We found the same association between these strong tidal currents and the rising tide when these motions are supposed to be stronger, i.e., during spring tides (Fig. 2). The lack of strong winds observed during samplings is also consistent with the known wind speed range at which these structures form and persist, i.e., not more than 10 m s^{-1} (Soloviev and Lukas 2014). Thermal stratification and the existence of an interface between warm surface waters and a cooler subthermocline layer are, however, required for internal wave generation and transmission (Helfrich and Pineda 2003). During our samplings, thermal vertical gradients were much lower (0.1°C m^{-1}, Fig. 3) than those measured in coastal waters off Southern California when conspicuous internal waves developed (0.9°C m^{-1}, Pineda 1999). The thermal values found during

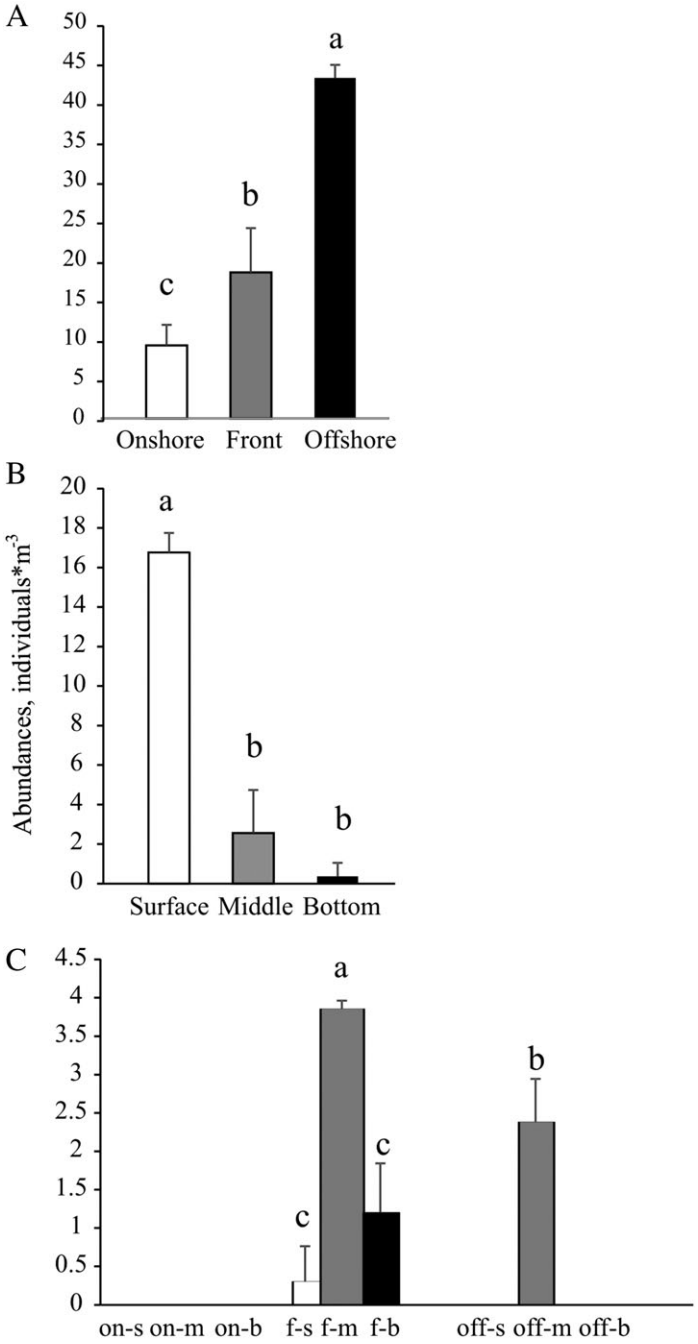

Fig. 6. Examples of larval distributions around nearshore frontal structures: (**A**) annelid segmented larvae at Event 1 after frontal development; (**B**) bryozoan cyphonauts at event 3 during frontal development; (**C**) balanid late nauplii at Event 2 during frontal development. Letters show significant groupings according to the corresponding analyses of variance, *see* Table 2 for levels of significance and acronyms in panel **C**.

this study are in the stratification range observed off Florida and California, when internal waves were also observed (Leichter et al. 1998; Noble et al. 2009; Ryan et al. 2014), although the typical Chl *a* maximum associated with the thermocline was marked in those studies, but not in our samplings (Figs. 3, 4 and 5). Nevertheless, Largier (1994) observed internal tides and propagation of slicks over the shelf off Cape Town when the water column was less stratified (around 0.04°C m^{-1}) and hypothesized that, under the proper topographic characteristics, the internal tide can be enhanced by the resonance between several generation sites on the shelf break, despite a low thermal stratification background. Similarly, internal tides were detected off the Western coast of Scotland across slightly stratified water columns (0.02°C m^{-1}) and were thought to be intensified by coastal-trapped waves (Rippeth and Inall 2002). Coastal-trapped waves are known to propagate eastward along the Agulhas Bank (Schumann and Brink 1990) and could exert similar effects on the internal tide along this coast. Thus, the development of internal waves across slightly stratified water columns may have occurred during our samplings. In fact, this is the most plausible explanation for the slicks observed in the field and in LANDSAT images on Event 2 (Supporting Information). These images revealed a banded pattern in contrast, consisting in 5–6 lines separated approximately 100 m from each other. Similar structures have already been observed in detail off Monterey Bay in California using satellite imagery similar to the one used in our study and interpreted as wind rows or Langmuir cells (Ryan et al. 2010). Langmuir cells are also characterized by parallel foam lines caused by winds acting on surface waters, but zonal winds responsible of Ekman transport were not blowing during Event 2 (Fig. 3). If Langmuir circulation was occurring, only alongshore winds could have formed the shore parallel lines observed as these usually develop in parallel to wind direction, but alongshore wind speeds were close to zero on that particular date. Furthermore, these lines were observed moving onshore, and Langmuir foam lines are known to remain at fixed locations (Soloviev and Lukas 2014). LANDSAT images also revealed a different structure further offshore consistent in an alongshore single line that was not sampled during Event 2 (Supporting Information). Such a feature could correspond to a shear front due to flow separation at the tip of Cape Recife or to an upwelling shadow front (McCabe et al. 2006; Ryan et al. 2010).

Larval distributions affected by internal motions

Two modes of horizontal, landward transport of zooplankton mediated by internal waves have been described: surface accumulation at convergent slicks formed between the upwelled inshore and warmer offshore water masses (Shanks 1983; Pineda 1994, 1999; Vargas et al. 2004; Weidberg et al. 2014) and subthermocline transport by tidal currents during the next phase of wave development (Pineda 1991; Leichter et al. 1998). These two modes are not mutually exclusive, as surface and bottom transport of barnacle nauplii and crab zoeae, respectively, have been observed during opposite phases of internal wave development (Lievana MacTavish et al. 2016). Our data, however, clearly support the subthermocline transport mode and not surface accumulation at the front. Surface convergent flows were relatively weak or even

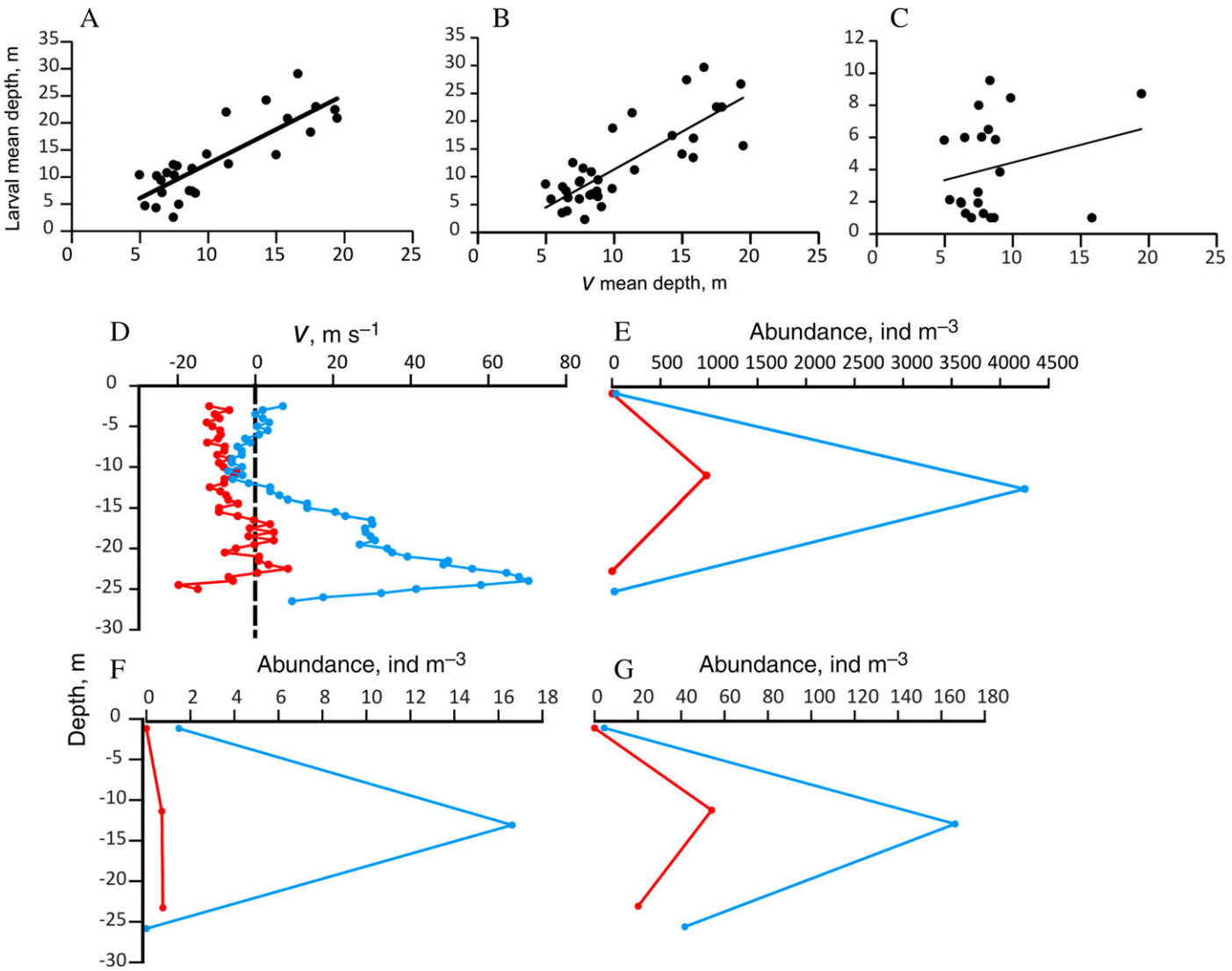

Fig. 7. Examples of OLS regressions between larval and meridional flow (*V*) mean depths for brachyuran zoeae (**A**, $R^2 = 0.69$, $p < 0.0001$), bivalve veligers (**B**, $R^2 = 0.65$, $p < 0.0001$) and bryozoan cyphonauts (**C**, $R^2 = 0.06$, $p = 0.28$). Vertical current profiles of *V* (**D**) and distributions of balanid early nauplii (**E**), chthamalid early nauplii (**F**) and gastropod veligers (**G**) are shown for the offshore station A during Event 1 in Times 1 and 2 (red and blue line, respectively). The dashed line shows the limit between shorewards and seawards flows in panel **D**. [Color figure can be viewed at wileyonlinelibrary.com]

negative (Table 1), thus failing to transport larvae to the front, while both strong surface convergent currents and planktonic aggregations have been found in other systems (Pineda 1999; Weidberg et al. 2014). On the other hand, much higher accumulation speeds were observed at the bottom layers during Time 2 for Events 1 and 2 (Table 1), as strong subthermocline shoreward flow occurred during the rising tide and after frontal development (Figs. 3, 4). These currents reached up to 90 cm s^{-1} (Figs. 3, 4) and may provide fast onshore advection of larvae at those depths. In agreement with these observations, both nearshore measurements and model simulations show that very strong currents can develop close to the bottom as internal waves shoal and break (Aghsaae et al. 2010; Richards et al. 2013).

Processes affecting nearshore larval distributions are often explored in a Lagrangian framework, assuming that internal waves may transport offshore larvae that were previously outside the domain sampled to the coast. An horizontal Eulerian perspective can however also be considered, assuming that most of the larvae sampled after the occurrence of the fronts were already there when the fronts were present and that the change in their distribution is not due to the arrival of offshore larvae, but to a shift in the vertical positioning of local larvae. In fact, our sampling design allows a comparison between larval abundances during and after the presence of fronts. Thus, for all the taxa which were located deeper in the water column at Time 2 for Events 1 and 2, larval abundances were overall not clearly higher in Time 2 compared to Time 1 (Table 2),

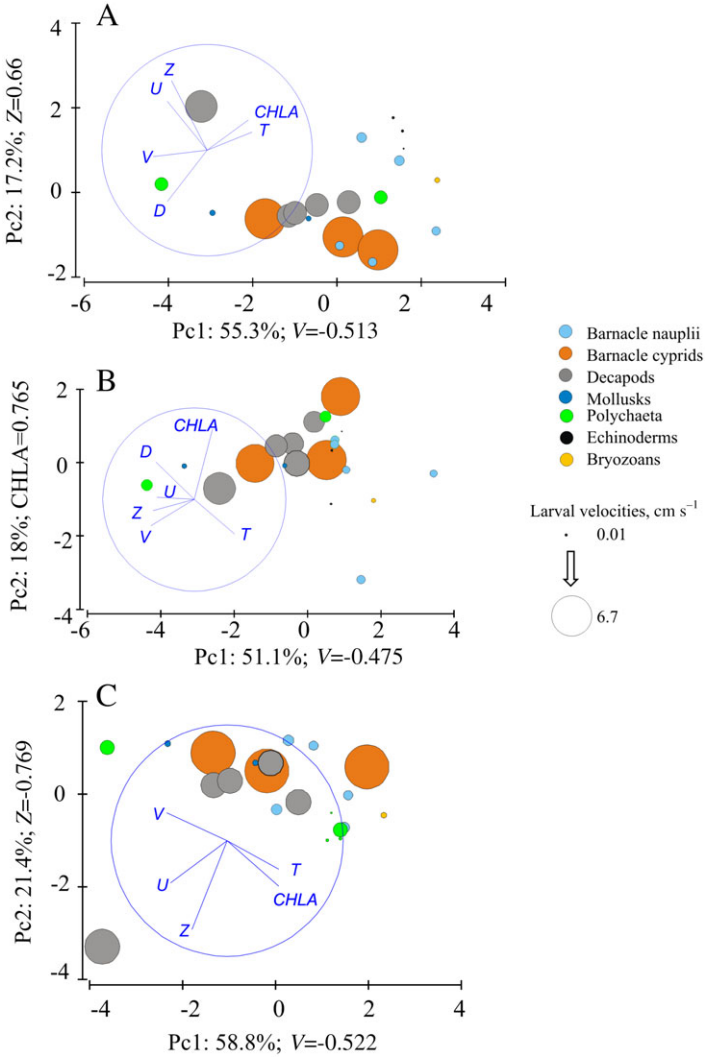

Fig. 8. PCA analyses for larval taxa for all samples (**A**), for time of frontal development, Time 1 (**B**), and after front occurrence, Time 2 (**C**). Each point represents a taxon, see legend for taxonomic groups and larval velocities. Percentage of variability is shown for each PC axis along with the linear coefficient of the most important variable (*T*, temperature; CHLA, Chl *a*; *U*, zonal flow; *V*, meridional flow; *Z*, vertical flow). [Color figure can be viewed at wileyonlinelibrary.com]

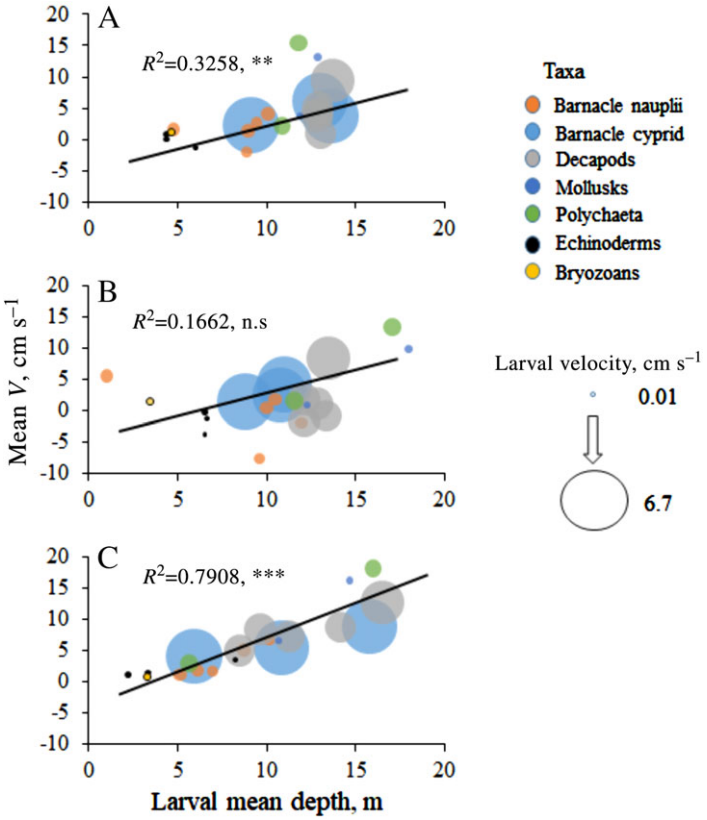

Fig. 9. Regressions between larval mean depth and mean cross-shore flows for all sampling occasions (**A**), during frontal development, Time 1 (**B**), and after frontal occurrence, Time 2 (**C**). Each dot is a taxon, see legend for general taxonomic groups and typical organismal velocities. Significance for regression is shown (*: $0.01 < p < 0.05$; **: $0.001 < p < 0.01$; ***: $p < 0.001$). [Color figure can be viewed at wileyonlinelibrary.com]

which points to a minor role of advection from outside our domain. More likely, the vertical distribution of local larvae was altered from Time 1 to Time 2. This perspective has been considered for holoplanktonic organisms at offshore waters, but also in lakes, where vertical oscillations of the pycnocline match vertical displacements of the distribution of the zooplankters (McManus et al. 2005; Rinke et al. 2007; Huber et al. 2011; van Haren 2014). Such a correspondence between larval vertical patterns and internal motions may indicate that the organisms are passively sinking and rising with the transmission of the internal waves. The physical data indicate that there was not a clear stratified water column with a pycnocline that larvae could follow passively (Figs. 3, 4 and 5) and, in fact, while the fronts were present on Events 1 and 2, most larval taxa were not at the surface, but evenly distributed in the vertical axis (Table 2). It was only after frontal occurrence that larvae sank and strong shoreward tidal currents developed. This points to active organismal behavior.

Active depth regulation in response to dynamic flows

The role of vertical migration in the spatial and temporal distributions of planktonic organisms has been described in many locations. The most studied type of migration observed in many different coastal and oceanic systems across multiple taxa is diel vertical migration. Our results point, however, to a more dynamic, flexible vertical migration in response to shoreward flows. Such behavior may not be incompatible with diel vertical migration given the highly adaptive nature of larval behavior across the water column, but it might prevail for coastal meroplankton under a contrasting vertical structure in cross-shore flow. The correspondence between larval mean depths and cross-shore flow vertical profiles (Fig. 7), the strong effect of these northward flows in structuring the larval

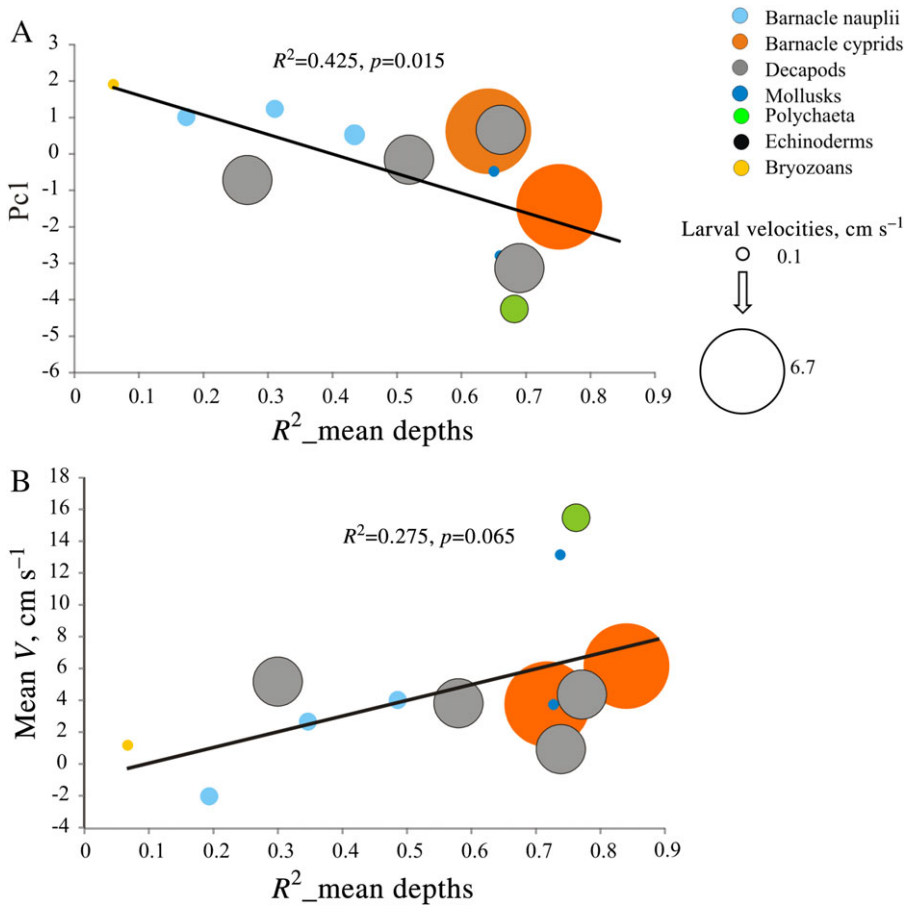

Fig. 10. Linear relationships of taxon-specific R^2 between larval and meridional flow mean depths with Pc1 score (**A**) and mean shorewards current velocities (**B**). Each dot is a taxon, see legend for general taxonomic groups and typical organismal velocities. [Color figure can be viewed at wileyonlinelibrary.com]

community, especially when they were fast and correlated with depth during Time 2 (Figs. 8, 9), and finally the association between larval community assemblages and the larval-onshore flow coupling for each taxon (Fig. 10) may indicate that these organisms were performing highly adaptable vertical movements in search of shoreward transport. Moreover, such adaptive behavior was successful in terms of onshore advection as those taxa exhibiting the best larval mean depth—shoreward mean depth couplings tended to experience stronger shoreward flows (Fig. 10B). From the perspective of selective pressure, behaviors enhancing the arrival of larvae at a relatively narrow and reduced adult habitat on the shore in a highly advective pelagic realm may be strongly favored and become more important than thermal and productivity characteristics of the water masses (Crisp 1976; Sulkin 1984; Naylor 2006). For larvae, in sharp contrast with pelagic holoplankton (Jackson and Strathmann 1981), to grow in productive waters with a suitable thermal range may not enhance survival if by the end of development they are not in the adult habitat on the coast. This is consistent with the fact that the distributions of mussel larvae over the Agulhas Bank were uncorrelated with temperature (Porri et al. 2014). In this context, the greater importance of cross-shore currents over environmental hydrographic variables is consistent with the selective pressures to which coastal meroplankton are subjected. In addition, complex behaviors that influence retention within those water layers moving onshore might have evolved. Certainly, when larval distributions were examined at the inshore waters with respect to the structure of cross-shore currents, the existence of such behaviors became clear for several taxa. Essentially, they consist of vertical migration against vertical currents under Ekman and tidal forcing (Cronin 1982; Queiroga and Blanton 2004; Genin et al. 2005; Shanks and Brinks 2005; Shanks and Shearman 2009). By opposing vertical currents, larvae would remain in those layers advected to the shore in each scenario. Nevertheless, during our cruises, vertical currents did not present a clear pattern across the water column (Figs. 3, 4 and 5). Biological rhythms in phase with the tide are less likely in our coastal site, as, in contrast with tidal channels and estuaries, the synchronization between barotropic and baroclinic tides at the open coast may not occur or may even be in opposite phase to the

expected (Leichter et al. 1998). This mismatch would make the evolution of internal biological synchronization to tides very unlikely outside of estuaries. Thus, the underlying mechanisms behind the association between larval and cross-shore currents vertical profiles remain unclear and they cannot be fully inferred from this observational field study. Further experimental work is required to directly evaluate larval vertical responses to contrasting flows under different physical conditions. The inclusion of coastal sound in such studies may be of particular interest, as it could be perceived by a wide range of zooplankters and it clearly indicates onshore direction (Rogers and Cox 1988; Radford et al. 2007; Lillis et al. 2014).

Role of swimming ability

Across surface frontal convergences, spatial gradients in the planktonic community can be observed driven by larval swimming speed with respect to horizontal and vertical convergent flows (Franks 1992; Pineda 1999; Hetland et al. 2002; Weidberg et al. 2014). Thus, relatively fast zooplankters may accumulate as they can oppose downward currents at the front, while slower organisms may sink and recirculate mainly toward the stratified side of the structure. Our results suggest, however, that swimming speed did not influence downward migration nor the degree of MLD-MVD coupling or larval community assemblages (Figs. 8, 9 and 10), probably because there was no persistent vertical flow opposing larval movement (Figs. 3, 4 and 5). This is in agreement with observations of larval transport by deep tidally driven shoreward flows, a process which affects different types of zooplankters, regardless of their swimming speeds (Pineda 1991; Leichter et al. 1998). On the other hand, at surface convergences, the water is forced downward at speeds that can overcome horizontal flows (Kilcher and Nash 2010; Weidberg et al. 2014) and can pose a constraint to larval motion, leading to spatial dislocation of populations based on relative swimming speed (Franks 1992).

Conclusions

During our coastal cruises, tidally forced internal wave dynamics were observed despite low levels of thermal stratification. The role of larval onshore transport by surface fronts was minor compared to that driven by strong deep shoreward currents during the opposite phase of the baroclinic internal tide. The clear association of many different larval taxa with these flows most likely indicates an active, finely tuned migration pattern through the water column which may allow landward transport, at least for local larvae from the inner shelf to the offshore side of the surf zone. In contrast to surface convergences, larval swimming speed was not related to this process and it occurred during the phase of the internal tide when surface fronts were not present. In order to infer the role of internal tidally forced motions in larval transport, the measurement of frequency, strength and persistence of surface manifestations of fronts, as foam lines or slicks, is of at least the same relevance as a full characterization of these deep shoreward, postfrontal currents.

References

Aghsaae, P., L. Boegman, and K. G. Lamb. 2010. Breaking of shoaling internal solitary waves. J. Fluid Mech. **659**: 289–317. doi:10.1017/S002211201000248X

Bakun, A. 1973. Coastal upwelling índices, west coast of North America, 1946–1971. NOAA technical report. US Department of Commerce. NMFS SSRF-671.

Barham, E. G. 1963. Siphonophores and the deep scattering layer. Science **140**: 826–828. doi:10.1126/science.140.3568.826

Chia, F. S., J. Buckland-Nicks, and C. M. Young. 1984. Locomotion of marine invertebrate larvae: A review. Can. J. Zool. **62**: 1205–1222. doi:10.1139/z84-176

Clarke, K. R., and R. N. Gorley. 2006. PRIMER v6: User manual/tutorial. PRIMER-E.

Crisp, D. J. 1976. Settlement responses in marine organisms, p. 83–124. *In* R. C. Newell [ed.], Adaptation to environment. Butterworths.

Cronin, T. W. 1982. Estuarine retention of larvae of the crab *Rhithropanopeus harrisii*. Estuar. Coast. Shelf Sci. **15**: 207–220. doi:10.1016/0272-7714(82)90028-2

Enright, J. T. 1977. Diurnal vertical migration: Adaptive significance and timing. Part 1. Selective advantage: A metabolic model. Limnol. Oceanogr. **222**: 856–872. doi:10.4319/lo.1977.22.5.0856

Fornshell, J. A., and A. Tesei. 2013. The development of SONAR as a tool in marine biological research in the twentieth century. Int. J. Oceanogr. **2013**: 1–9. doi:10.1155/2013/678621

Franks, P. J. S. 1992. Sink or swim: Accumulation of biomass at fronts. Mar. Ecol. Prog. Ser. **82**: 1–12. doi:10.3354/meps082001

Genin, A., S. J. Jaffe, R. Reef, C. Richter, and P. J. S. Franks. 2005. Swimming against the flow: A mechanism of zooplankton aggregation. Science **308**: 860–862. doi:10.1126/science.1107834

Goschen, W. S., and E. H. Schumann. 1990. Agulhas Current variability and inshore structures off the Cape Province. S. Afr. J. Geophys. Res. **95**: 667–678. doi:10.1029/JC095iC01p00667

Goschen, W. S., T. G. Bornman, S. H. P. Deyzel, and E. H. Schumann. 2015. Coastal upwelling on the far eastern Agulhas Bank associated with large meanders in the Agulhas Current. Cont. Shelf Res. **101**: 34–46. doi:10.1016/j.csr.2015.04.004

Hays, G. C., H. Kennedy, and B. W. Frost. 2001. Individual variability in diel vertical migration of a marine copepod: Why some individuals remain at depth when others migrate. Limnol. Oceanogr. **46**: 2050–2054. doi:10.4319/lo.2001.46.8.2050

Helfrich, K. R., and J. Pineda. 2003. Accumulation of particles in propagating fronts. Limnol. Oceanogr. **48**: 1509–1520. doi:10.4319/lo.2003.48.4.1509

Hetland, R. D., D. J. McGillicuddy, and R. P. Signell. 2002. Crossfrontal entrainment of plankton into a buoyant plume: The frog tongue mechanism. J. Mar. Res. **60**: 763–777. doi:10.1357/002224002321505129

Heywood, K. 1996. Diel vertical migration of zooplankton in the Northeast Atlantic. J. Plankton Res. **18**: 163–184. doi:10.1093/plankt/18.2.163

Holloway, P. E. 1987. Internal hydraulic jumps and solitons at a shelf break region on the Australian north west shelf. J. Geophys. Res. **92**: 5405–5416. doi:10.1029/JC092iC05p05405

Hsu, S. A., E. A. Meindl, and D. B. Gilhousen. 1994. Determining the power-lawwind-profile exponent under near-neutral stability conditions at sea. J. Appl. Meteorol. **33**: 757–765. doi:10.1175/1520-0450(1994)033<0757:DTPLWP>2.0.CO;2

Huber, A. M. R., F. Peeters, and A. Lorke. 2011. Active and passive vertical motion of zooplankton in a lake. Limnol. Oceanogr. **56**: 695–706. doi:10.4319/lo.2011.56.2.0695

Jackson, G. A., and R. R. Strathmann. 1981. Larval mortality from offshore mixing as a link between precompetent and competent periods of development. Am. Nat. **118**: 16–26. doi:10.1086/283797

Jackson, J. M., L. Rainville, M. J. Roberts, C. D. McQuaid, and J. R. E. Lutjeharms. 2012. Mesoscale bio-physical interactions between the Agulhas Current and the Agulhas Bank, South Africa. Cont. Shelf Res. **49**: 10–24. doi:10.1016/j.csr.2012.09.005

Kilcher, L. F., and D. J. Nash. 2010. Structure and dynamics of the Columbia River tidal plume front. J. Geophys. Res. **115**: C05S90. doi:10.1029/2009JC006066

Lagos, N. A., J. C. Castilla, and B. R. Broitman. 2008. Spatial environmental correlates of intertidal recruitment: A test using barnacles in Northern Chile. Ecol. Monogr. **78**: 245–261. doi:10.1890/07-0041.1

Largier, J. L. 1993. Estuarine fronts: How important are they? Estuaries **16**: 1–11. doi:10.2307/1352760

Largier, J. L. 1994. The internal tide over the shelf inshore of Cape Point Valley, South Africa. J. Geophys. Res. **99**: 10023–10034. doi:10.1029/93JC03220

Largier, J. L., and V. P. Swart. 1987. East–west variation in thermocline break-down on the Agulhas Bank. S. Afr. J. Mar. Sci. **5**: 263–272. doi:10.2989/025776187784522252

Le Fevre, J. 1986. Aspects of the biology of frontal systems, 1st ed. Univ. de Bretagne Occidentale.

Leichter, J. J., G. Shellenbarger, J. S. Genovese, and S. R. Wing. 1998. Breaking internal waves on a Florida (USA) coral reef: A plankton pump at work? Mar. Ecol. Prog. Ser. **166**: 83–97. doi:10.3354/meps166083

Lievana MacTavish, A., L. B. Ladah, M. F. Lavin, A. Filonov, F. J. Tapia, and J. Leichter. 2016. High frequency (hourly) variation in vertical distribution and abundance of meroplanktonic larvae in nearshore waters during strong internal tidal forcing. Cont. Shelf Res. **117**: 92–99. doi:10.1016/j.csr.2016.02.004

Lillis, A., D. B. Eggleston, and D. R. Bohnenstiehl. 2014. Estuarine soundscapes: Distinct acoustic characteristics of oyster reefs compared to soft-bottom hábitats. Mar. Ecol. Prog. Ser. **505**: 1–17. doi:10.3354/meps10805

Lutjeharms, J. R. E. 2006. The Agulhas Current. Springer.

Lutjeharms, J. R. E., J. Cooper, and M. J. Roberts. 2000. Upwelling at the inshore edge of the Agulhas Current. Cont. Shelf Res. **20**: 737–761. doi:10.1016/S0278-4343(99)00092-8

McCabe, R. M., P. MacCready, and G. Pawlak. 2006. Form drag due to flow separation at a headland. J. Phys. Oceanogr. **36**: 2136–2152. doi:10.1175/JPO2966.1

McManus, M. A., O. M. Cheriton, P. J. Drake, D. V. Holliday, C. D. Storlazzi, P. L. Donaghay, and C. E. Greenlaw. 2005. The effects of physical processes on the structure and transport of thin zooplankton layers in the coastal ocean. Mar. Ecol. Prog. Ser. **301**: 199–215. doi:10.3354/meps301199

McQuaid, C. D., and T. E. Phillips. 2000. Limited wind-driven dispersal of intertidal mussel larvae: In situ evidence from the plankton and the spread of the invasive species *Mytilus galloprovincialis* in South Africa. Mar. Ecol. Prog. Ser. **201**: 211–220. doi:10.3354/meps201211

Naylor, E. 2006. Orientation and navigation in coastal and estuarine zooplankton. Mar. Freshw. Behav. Physiol. **39**: 13–24. doi:10.1080/10236240600593344

Noble, M., B. Jones, P. Hamilton, J. Xu, G. Robertson, L. Rosenfeld, and J. Largier. 2009. Cross-shelf transport into nearshore waters due to shoaling internal tides in San Pedro Bay, CA. Cont. Shelf Res. **29**: 1768–1785. doi:10.1016/j.csr.2009.04.008

Pineda, J. 1991. Predictable upwelling and the shoreward transport of planktonic larvae by internal tidal bores. Science **253**: 548–551. doi:10.1126/science.253.5019.548

Pineda, J. 1994. Internal tidal bores in the nearshore: Warm-water fronts, seaward gravity currents and the onshore transport of neustonic larvae. J. Mar. Res. **52**: 427–458. doi:10.1357/0022240943077046

Pineda, J. 1999. Circulation and larval distribution in internal tidal bore warm fronts. Limnol. Oceanogr. **44**: 1400–1414. doi:10.4319/lo.1999.44.6.1400

Pond, S., and G. L. Pickard. 1983. Introductory dynamical oceanography. Pergamon Press.

Porri, F., J. M. Jackson, C. E. O. von der Meden, N. Weidberg, and C. D. McQuaid. 2014. The effect of mesoscale oceanographic features on the distribution of mussel larvae along the south coast of South Africa. J. Mar. Syst. **132**: 162–173. doi:10.1016/j.jmarsys.2014.02.001

Queiroga, H., and J. O. Blanton. 2004. Interactions between behaviour and physical forcing in the control of horizontal transport of decapod crustacean larvae: An overview. Adv. Mar. Biol. **47**: 107–214.

Radford, C. A., A. G. Jeffs, and J. C. Montgomery. 2007. Directional swimming behavior by five species of crab postlarvae in response to reef sound. Bull. Mar. Sci. **80**: 369–378.

Richards, C., D. Bourgault, P. S. Galbraith, A. Hay, and D. E. Kelley. 2013. Measurements of shoaling internal waves and turbulence in an estuary. J. Geophys. Res. Oceans **118**: 273–286. doi:10.1029/2012JC008154

Rinke, K., I. Hübner, T. Petzoldt, S. Rolinski, M. Konig-Rinke, J. Post, A. Lorke, and J. Benndorf. 2007. How internal waves influence the vertical distribution of zooplankton. Freshw. Biol. **52**: 137–144. doi:10.1111/j.1365-2427.2006.01687.x

Rippeth, T. P., and M. E. Inall. 2002. Observations of the internal tide and associated mixing across the Malin Shelf. J. Geophys. Res. **107**: 3028. doi:10.1029/2000JC000761

Rogers, P. H., and M. Cox. 1988. Underwater sound as a biological stimulus, p. 131–149. *In* J. Atema, R. R. Fay, A. N. Popper, and W. N. Tavolga [eds.], Sensory biology of aquatic animals. Springer-Verlag.

Ryan, J. P., and others. 2010. Recurrent frontal slicks of a coastal ocean upwelling shadow. J. Geophys. Res. Oceans **115**: C12070. doi:10.1029/2010JC006398

Ryan, J. P., J. B. J. Harvey, Y. Zhang, and C. B. Woodson. 2014. Distributions of invertebrate larvae and phytoplankton in a coastal upwelling system retention zone and peripheral front. J. Exp. Mar. Biol. Ecol. **459**: 51–60. doi:10.1016/j.jembe.2014.05.017

Schumann, E. H., L. A. Perris, and I. T. Hunter. 1982. Upwelling along the south coast of the Cape Province, South Africa. S. Afr. J. Mar. Sci. **78**: 238–242.

Schumann, E. H., and K. H. Brink. 1990. Coastal-trapped waves off the coast of South Africa: Generation, propagation and current structures. J. Phys. Oceanogr. **20**: 1206–1218. doi:10.1175/1520-0485(1990)020<1206:CTWOTC>2.0.CO;2

Shanks, A. L. 1983. Surface slicks associated with tidally forced internal waves may transport pelagic larvae of benthic invertebratesand fishes shoreward. Mar. Ecol. Prog. Ser. **13**: 311–315. doi:10.3354/meps013311

Shanks, A. L., J. L. Largier, L. Brink, J. Brubaker, and R. Hoof. 2000. Demonstration of the onshore transport of larval invertebrates by the shoreward movement of an upwelling front. Limnol. Oceanogr. **45**: 230–236. doi:10.4319/lo.2000.45.1.0230

Shanks, A. L., A. McCulloch, and J. Miller. 2003. Topographically generated fronts, very nearshore oceanography and the distribution of larval invertebrates and holoplankters. J. Plankton Res. **25**: 1251–1277. doi:10.1093/plankt/fbg090

Shanks, A. L., and L. Brinks. 2005. Upwelling, downwelling, and cross-shelf transport of bivalve larvae: Test of a hypothesis. Mar. Ecol. Prog. Ser. **302**: 1–12. doi:10.3354/meps302001

Shanks, A. L., and R. K. Shearman. 2009. Paradigm lost? Cross-shelf distributions of intertidal invertebrate larvae are unaffected by upwelling or downwelling. Mar. Ecol. Prog. Ser. **385**: 189–204. doi:10.3354/meps08043

Soloviev, A., and R. Lukas. 2014. The near-surface layer of the ocean structure, dynamics and applications. Springer.

Stich, H. B., and W. Lampert. 1981. Predator evasion as an explanation of diurnal vertical migration by zooplankton. Nature **293**: 396–398. doi:10.1038/293396a0

Sulkin, S. D. 1984. Behavioural basis of depth regulation in the larvae of brachyuran crabs. Mar. Ecol. Prog. Ser. **15**: 181–205. doi:10.3354/meps015181

Tapia, F. J., C. DiBacco, J. Jarrett, and J. Pineda. 2010. Vertical distribution of barnacle larvae at a fixed nearshore station in southern California: Stage-specific and diel patterns. Estuar. Coast. Shelf Sci. **86**: 265–270. doi:10.1016/j.ecss.2009.11.003

van Haren, H. 2014. Internal wave–zooplankton interactions in the Alboran Sea (W-Mediterranean). J. Plankton Res. **36**: 1124–1134. doi:10.1093/plankt/fbu031

Vargas, C. A., D. A. Narvaez, A. Piñones, R. M. Venegas, and S. A. Navarrete. 2004. Internal tidal bore warm fronts and settlement of invertebrates in Central Chile. Estuar. Coast. Shelf Sci. **61**: 603–612. doi:10.1016/j.ecss.2004.07.006

Weidberg, N., C. Lobón, E. López, L. García-Flórez, M. P. Fernández-Rueda, J. L. Largier, and J. L. Acuña. 2014. Effect of nearshore slicks on meroplankton distributions: Role of larval behaviour. Mar. Ecol. Prog. Ser. **506**: 15–30. doi:10.3354/meps10777

Weidberg, N., F. Porri, C. E. O. von der Meden, J. M. Jackson, W. Goschen, and C. D. McQuaid. 2015. Mechanisms of nearshore retention and offshore export of mussel larvae over the Agulhas Bank. J. Mar. Syst. **144**: 70–80. doi:10.1016/j.jmarsys.2014.11.012

Woodson, C. B., and others. 2012. Coastal fronts set recruitment and connectivity patterns across multiple taxa. Limnol. Oceanogr. **57**: 582–596. doi:10.4319/lo.2012.57.2.0582

Acknowledgments

The South African Weather Service provided valuable wind data. We thank Rachel Ndhlovu for her work in larval identification and the captain and crew of the RV *uKwabelana*, Ryan Palmer, Jacqui Trasierra, Shana Mian, Olwethu Duna, Carlota Fernández for assistance and data collection. This research was funded by the African Coelacanth Ecosystem Programme (ACEP III) and it is supported by the South African Research Chairs Initiative of the Department of Science and Technology, the National Research Foundation, and the South African Institute for Aquatic Biodiversity.

Conflict of Interest

None declared.

Submitted 16 April 2018
Revised 24 August 2018
Accepted 08 October 2018

Associate editor: James Leichter